Improving Pt Catalyst Durability and Activity for H_2 and O_2 Reactions by N-Doping of Graphene and SWCNTs

M.N. Groves[1], A. Chan[1], C. Malardier-Jugroot[1] and M. Jugroot[2]

[1]Department of Chemistry and Chemical Engineering
[2]Department of Mechanical Engineering
Royal Military College of Canada, Kingston, ON, Canada
michael.groves@rmc.ca, cecile.malardier-jugroot@rmc.ca

ABSTRACT

Improving the efficiency and durability of Pt catalysts for the Hydrogen Evolution Reaction (HER) and Oxygen Reduction Reaction (ORR) are key components for the commercialization of proton exchange membrane fuel cells (PEMFC). This work uses Density Functional Theory (DFT) to investigate improvements to these two key reactions by doping graphene and single walled carbon nanotubes (SWCNTs) with Nitrogen. It was found that the binding energy can increase by a factor of two between undoped and N-doped systems. Furthermore, a decrease in the magnitude of ΔG_{ad} by a factor of ten and 1.16 was measured between undoped and N-doped systems for the HER and ORR respectively.

Keywords: single walled carbon nanotubes, density functional theory, platinum catalyst, nitrogen doping, hydrogen evolution reaction, oxygen reduction reaction

1 INTRODUCTION

Developing alternative low carbon intensive energy systems are important for both curbing the human influence on climate change and diversifying energy sources. The proton exchange membrane fuel cell promises to be one such source. Unfortunately, there are still barriers in terms of cost and durability that prevent widespread utilization. Pt based catalysts are still found to be the most chemically active for this application so minimizing Pt loading while maintaining catalytic activity is key.

It has be demonstrated that nitrogen doped carbon supports can increase the durability and activity of a catalyst [1], [2]. This study uses density functional theory (DFT) to calculate the binding energy between nitrogen doped carbon structures, such as graphene and single walled carbon nanotubes (SWCNT) and a lone Pt atom. These same systems were then optimized again with a single Pt atom and both H_2 and O_2 to determine the change in Gibbs free energy of absorption (ΔG_{ad}). This has been shown to be a good indicator of activity of a catalyst where the closer ΔG_{ad} is to zero the more active the catalyst [3].

2 COMPUTATIONAL PROCEDURE

All results have been have been found using the Gaussian 03 software package either on a native Mac OS X Leopord system using Gaussian 03 Revision E.01, or using the High Performance Computer Virtual Laboratory (HPCVL) using Gaussian 03 Revision C.02[4]. DFT was used to create two sets of data with two different basis sets. Lanl2DZ, uses D95V for first row atoms [5] and the Los Alamos effective core potential plus DZ on Na-La and Hf-Bi [6]–[8]. Lanl2MB, the second basis set employed, uses STO-3G for first row atoms [9], [10] and the Los Alamos effective core potential plus MBS on Na-La and Hf-Bi [6]–[8]. The use of effective core potentials was necessary to handle the large number of electrons present in Pt atoms. The Lanl2DZ basis data is used for comparison between graphene systems only. The Lanl2MB basis set data is for comparison between SWCNT and graphene systems as it is less costly computationally without loss to qualitative trends. The B3LYP functional was used for all cases [11].

The pure graphene surface is constructed with 42 C atoms and 16 H atoms. Each dopant replaces one C atom in the lattace. Positioning of the dopants was done with the intention to create a symmetric plane to minimize the number of scan coordinates for a potential energy surface scan. These substrates were first geometrically optimized using the Lanl2MB basis set followed by a second geometry optimization using the Lanl2DZ basis set. Next, a potential energy scan of a Pt atom over the Lanl2MB geometry optimized surface was performed using the Lanl2MB basis set. This was used to determine the starting location of the Pt for the ensuing geometry optimization. A geometry optimization of the Pt over the substrate was first done using Lanl2MB and followed by a second one with the Lanl2DZ basis set. In addition to this, a Pt atom was geometrically optimized using both the Lanl2MB and Lanl2DZ basis sets. The binding energy (E_B) between the Pt and the substrate can then be calculated from

$$E_B = E(Pt/substrate) - E(substrate) - E(Pt) \quad (1)$$

where $E(Pt/substrate)$ is the total energy of the Pt / substrate geometry optimization, $E(substrate)$ is the total energy of the substrate geometry optimization, and

$E(Pt)$ is the total energy from a Pt atom geometry optimization. All of these energies are always taken from simulations using the same basis set.

For the ΔG_{ad} of H_2 and O_2, a geometry optimization, first with the Lanl2MB basis set followed by the Lanl2DZ basis set, is completed with the Pt / substrate / gas molecule ensemble. A frequency calculation is then done on both the Lanl2MB and Lanl2DZ optimized systems of the Pt / substrate, gas molecule, and Pt / substrate / gas molecule systems to evaluate the thermodynamic properties of the system. The ΔG_{ad} of a specified gas is then calculated to be

$$\begin{aligned} \Delta G_{ad} &= G_{Pt/substrate/gas} \\ &\quad -G_{Pt/substrate} - G_{gas} \end{aligned} \tag{2}$$

where $G_{Pt/substrate/gas}$, $G_{Pt/substrate}$ and G_{gas} are the Gibbs free energy calculated at 0°K for the Pt / substrate / gas, Pt / substrate, and gas systems respectively.

The pure SWCNTs were constructed using 112 C atoms and 32 H atoms. The length of the SWCNT is 7.43Å with a diameter of 11.33Å and arranged in an armchair pattern. This is when the components of the chirality vector, defined by the unit vectors of the hexagonal honeycomb lattice, have the same magnitude ($\vec{C} = n\hat{a_1} + m\hat{a_2}, n = m$). In this case (8,8) SWCNTs are used. It can be shown that these SWCNT demonstrate metallic conducting properties which would be useful in moving electrons to and from the catalyst site [12]. To determine the binding energy between a Pt atom and a SWCNT substrate, the same procedure is followed as before from the graphene substrate cases. For these systems only the Lanl2MB basis set is used. For the SWCNT systems the number of atoms have almost tripled and as a result a less computationally costly basis set is necessary.

3 RESULTS AND DISCUSSION

3.1 Binding Energy of Pt on Graphene and SWCNTs

In addition to an undoped graphene surface, five Nitrogen doped graphene substrates were used: a single Nitrogen doped surface, three two Nitrogen doped surfaces with N-N distances of 2.50Å , 3.79Å and 5.16Å respectively, and a graphene sheet where a quarter of the Carbon atoms are replaced with Nitrogen atoms equally distributed over the surface. An example of the potential energy surface for the 3.79Å two Nitrogen doped system with a Pt atom scanning 2.3Å above the substrate can be seen in figure 1. A ball and stick diagram of the same system with a box outlining the scanned area can be seen in figure 2. This shows that the most favourable location for the Pt to bind is equally over the

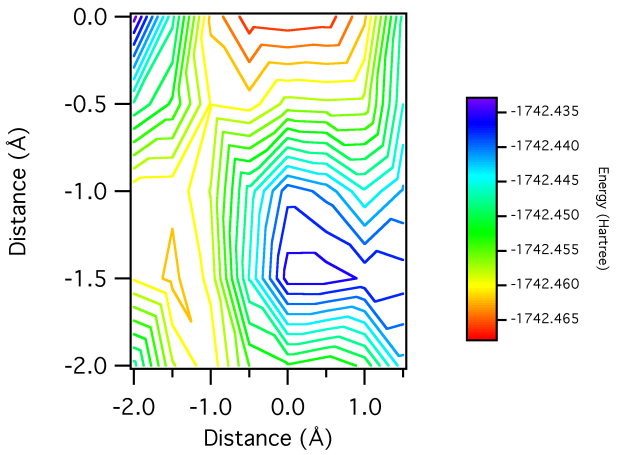

Figure 1: Potential energy surface of the 3.79Å two Nitrogen doped system with a Pt atom scanning 2.3Å above the substrate.

two Carbon atoms between the Nitrogen atoms as it has the lowest potential energy. As stated before, this was done with all the substrates to determine the starting point for the geometry optimization.

The results for the geometry optimization using the Lanl2DZ basis set on the graphene substrates can be seen in figure 3. The undoped graphene surface shows the weakest binding energy at −1.271eV. This is consistent with other values in the literature [13], [14]. The quarter N-doped graphene surface shows the strongest binding energy at −2.521eV with the 2.50Å two N-N doped graphene close behind at −2.510eV.

Looking at the natural bond orbital output [15] for the three, two Nitrogen-doped graphene substrate systems shows an increase in electron density in the valence band of the Pt and a decrease in the valence band and natural charge in the N's as the N-N distance decreases. In addition to this, the total number of orbitals that interact to bind the Pt to the surface also decreases as the N-N distance decreases. It seems that the proximity of the Nitrogens aids them in donating charge and helps localize the electrons that the Pt and C atoms share. In addition to this, the C atoms that the Pt directly interacts with also show an increase in natural charge as well as a decrease in electron density in their valence band as the N-N distance decreases. This also demonstrates the stabilizing effect the N atoms have over the C atoms which allows them to bond more strongly to the Pt.

Comparing these results with a recent publication by Acharya *et al.* [16] probably demonstrates the necessity of using geometrically optimized systems instead of the PES to calculate binding energies. In their work they show that a Boron-doped surface similar to the one seen in figure 2 shows a higher binding energy with Pt than the N-doped analogue. This is confirmed when com-

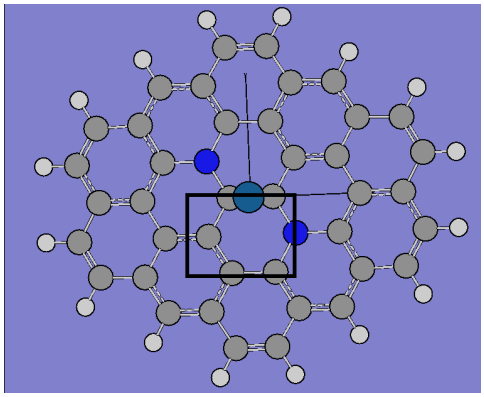

Figure 2: Ball and stick diagram of the 3.79Å two Nitrogen (shown in dark blue) doped system with a Pt atom (shown in light blue) 2.3Å above the substrate (C is grey and H is white). The black box represents the scanned area the Pt atom covers ($-2.0\text{Å} \leq x \leq 1.5\text{Å}$, $-2.0\text{Å} \leq y \leq 0\text{Å}$).

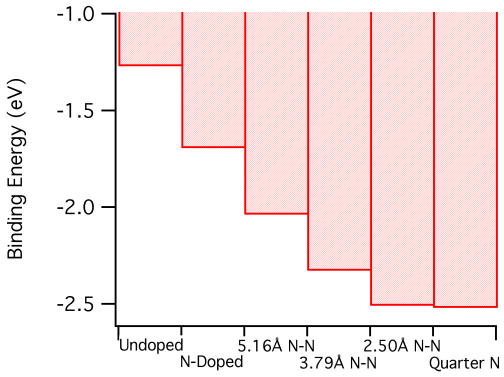

Figure 3: Pt binding energy to N-doped graphene surfaces using the Lanl2DZ basis set.

paring our PES scan of a 3.79Å B-B doped graphene surface with a Pt 2.3Å above its surface with the results from figure 1. However, when a geometry optimization is performed the binding energy was determined to be -2.255eV for the 3.79Å B-B doped substrate with Pt. This is weaker than the -2.328eV binding energy measured in the 3.79Å N-N doped case. In the geometry optimization, the Pt atom interacts with the substrate atoms which changes their positions as well as re-order molecular orbitals. This does not occur in a PES and probably demonstrates the importance of performing a geometry optimization when determining values like binding energy.

The SWCNTs were doped in the same way as the graphene substrates were in order to directly compare them however, only undoped, 3.79Å N-N doped, 2.50Å N-N doped and quarter N doped versions were evaluated. Table 1 shows the results from those simulations using the Lanl2MB basis set. As demonstrated here and in the literature [17], it is more favourable for the Pt to be on the outside of a SWCNT than on graphene or the inside. Our results of the undoped case are consistent with those found in Chen *et al.* [17]. Zhang *et al.* reported that coiling a graphene sheet into a SWCNT will cause a strain due to the curvature which induces a charge redistribution of the conjugate π bonds. Charges located initially on the inside will repel each other and migrate to the outside facilitating greater bond strength there and reducing it on the inside [18]. The binding energy seems to increase in strength on the outside of the SWCNT the greater the radius of curvature implying that more charge has migrated through conduction from the inside to the outside [17].

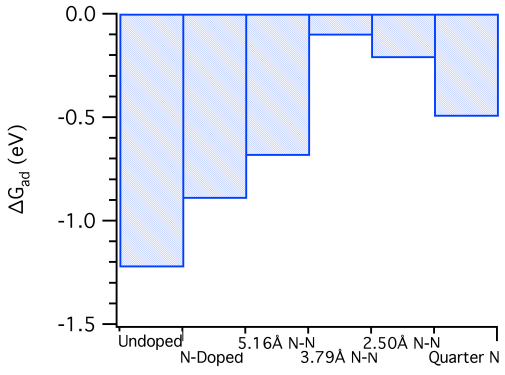

Figure 4: ΔG_{ad} of H_2 on graphene using the Lanl2DZ basis set.

This same effect was seen for every N-doped SWCNT where the Pt was bonded to the outside, inside and to a flat graphene surface. This indicates that the N-atoms do not affect the migration of charge from inside to outside. In addition to this, the benefit to the binding energy was seen in the SWCNTs as it was in the graphene sheets implying that N-doped SWCNTs, particularly quarter N-doped tubes, could make a more durable Pt catalyst support than undoped SWCNTs or graphene sheets.

3.2 ΔG_{ad} of H_2 and O_2 on Graphene

The results for the ΔG_{ad} of H_2 on graphene can be seen in figure 4. According to these results, there is not a direct relationship between binding energy between the surface and the Pt and catalytic activity of the Pt absorbing H_2. The 3.79Å N-N doped graphene surface shows the most promise for the best performing catalyst substrate with a ΔG_{ad} of H_2 of $-0.106eV$. This is more than a factor of 10 difference over an undoped graphene surface which has a ΔG_{ad} of H_2 of $-1.226eV$.

A similar yet less dramatic relationship is seen in

Doping	Pt Outside SWCNT (eV)	Graphene (eV)	Pt Inside SWCNT (eV)
None	−2.428	−1.975	−1.542
3.79Å N-N	−3.680	−3.224	−2.697
2.50Å N-N	−4.168	−3.719	−3.442
Quarter N	−4.207	−4.135	

Table 1: Binding energy results between Pt atoms and N-doped SWCNTs using the Lanl2MB basis set. The corresponding graphene substrate data is provided evaluated with the Lanl2MB basis set for reference. The Quarter N binding energy for 1 Pt inside the SWCNT had not finished evaluating at the time of publication but it is expected to be less than the 1 Pt Outside and Graphene case.

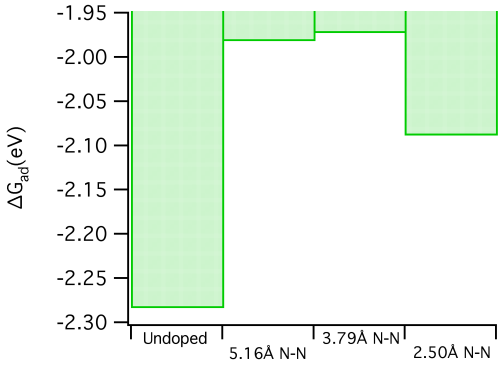

Figure 5: ΔG_{ad} of O_2 on graphene using the Lanl2DZ basis set. The single N-Doped and Quarter N-doped substrates had not finished being evaluated at the time of publication but is expected to have a similar relationship to the ΔG_{ad} of H_2 with the other substrates.

the ΔG_{ad} of O_2 data as seen in figure 5. Again, the most promising catalyst support is the 3.79Å N-N doped graphene surface with a ΔG_{ad} of O_2 of $-1.973eV$. This is only a factor 1.16 difference between the undoped graphene surface which has a ΔG_{ad} of O_2 of $-2.284eV$.

4 CONCLUSION

It has been shown using DFT that N-doping of carbon structures can increase both the durability and catalytic activity of Pt catalysts for the HER and ORR. The binding energy between the Pt and the C substrate increases with the number and proximity of N-dopants as well as the curvature of the structure provided that the Pt is on the outside. As for the activity of the Pt catalyst, a ten-fold reduction in magnitude of ΔG_{ad} of H_2 was seen between the undoped case and the 3.79Å N-N doped graphene surface, while a modest factor of 1.16 was seen between the same two systems. Future work will focus on the ΔG_{ad} of H_2 and O_2 on the SWCNT systems and their further potential improvements to these reactions as well as exploring the reason for these improvements.

REFERENCES

[1] Y. Shao, G. Yin, and Y. Gao, J. Power Sources, 171, 558 2007.

[2] B. Wang, J. Power Sources 152, 1, 2005.

[3] J. Greely, T. Jaramillo, J. Bonde, I. Chorkendorff, and J. Norskov, Nature Materials, 5, 909, 2006.

[4] Gaussian 03, M. J. Frisch *et al.*, Gaussian, Inc., Wallingford CT, 2004.

[5] T. H. Dunning Jr. and P. J. Hay, "Modern Theoretical Chemistry," Ed. H. F. Schaefer III, Vol. 3, Plenum, 1-28, 1976.

[6] P. J. Hay and W. R. Wadt, J. Chem. Phys. 82, 270, 1985.

[7] W. R. Wadt and P. J. Hay, J. Chem. Phys. 82, 284, 1985.

[8] P. J. Hay and W. R. Wadt, J. Chem. Phys. 82, 299, 1985.

[9] W. J. Hehre, R. F. Stewart, and J. A. Pople, J. Chem. Phys. 51, 2657, 1969.

[10] J. B. Collins, P. v. R. Schleyer, J. S. Binkley, and J. A. Pople, J. Chem. Phys. 64, 5142, 1976.

[11] A. D. Becke, J. Chem. Phys. 98, 5648, 1993.

[12] P. Avouris, and J. Chen, Materials Today, 9, 46, 2006.

[13] A. Maiti, and A. Ricca, Chem. Phys. Lett. 395, 7, 2004.

[14] D. H. Chi, N. T. Cuong, N. A. Tuan, Y.-T. Kim, H. T. Bao, T. Mitani, T. Ozaki, and H. Nagaoc, Chem. Phys. Lett. 432, 213, 2006.

[15] A. E. Reed, L. A. Curtiss, and F. Weinhold, Chem. Rev. 88, 899, 1988.

[16] C. K. Acharya, D. I. Sullivan, and C. H. Turner, J. Phys. Chem. 112, 13607, 2008.

[17] G. Chen, and Y. Kawazoe, Phys. Rev. B. 73, 125410, 2006.

[18] Y. Zhang, and H. Dai, Appl. Phys. Lett. 77, 3015, 2000.